Armenian Journal of Physics, 2017, vol. 10, issue 4, pp. 128-143

Stopping power and the straggling parameter of a heavy charged particle moving through a homogeneous free-electron gas

H.H. Matevosyan[1], K.A. Sargsyan[1], H.F. Haroyan[2]

[1]*Department of Theoretical Physics, Institute of Radiophysics and Electronics, 0203 Ashtarak, Armenia*
[2]*Yerevan State University, Alex Manoogian 1, 0025, Yerevan, Armenia*

Received 25 February 2017

Abstract. The mean free path, the electronic stopping power and the straggling parameter of a heavy charged particle moving through a homogeneous free-electron gas are addressed in the low-velocity regime and within the dielectric formalism using the Lindhard dielectric function. Simple analytical formulas are developed for these macroscopic cross sections, which are more accurate in the whole electron density range than those proposed to date by some authors.

Keywords: macroscopic cross sections; friction coefficients; dielectric formalism; local-plasma approximation

1. Introduction

The energy loss of swift charged particles moving in a degenerate electron gas is of fundamental importance in many fields of science and technology in order to understand the basic properties of their slowing down in real solids. Perturbative and non-perturbative theoretical models have been devised over the years to investigate the dependence of the electronic stopping power, and other macroscopic cross sections (MCSs) like the inverse mean free path and the straggling parameter, on the projectile charge and velocity, as well as on the properties of the traversed medium[1,2].

The dielectric formalism in the random-phase approximation [1,3] is a perturbative theoretical framework that has been extensively used to model the energy loss of charged particles in condensed matter (see e.g. [1,2] for reviews). This formalism accounts for the basic features of a homogeneous free electron gas (FEG) such as the creation of electron-hole pairs and the spectrum of collective (plasmon) excitations [1,3]. However, the electronic density encountered by a projectile along its trajectory in a real solid is seldom constant. The local plasma approximation (LPA) offers a sensible manner to handle the problem of an inhomogeneous electron density: each volume element of the medium is regarded as an independent homogeneous FEG. Then, a given MCS is expressed as a volume integral over the MCS evaluated at the local electron density in the solid.

In spite of its limitations, pointed out e.g. in [4], the LPA has been successfully employed in conjunction with the dielectric formalism (implemented through the Lindhard dielectric function) to calculate MCSs of charged particles in condensed media. For instance, this methodology is able to

describe quite accurately the stopping power of ions at random incidence [5-13], in channeling conditions [14] and in grazing incidence on surfaces [15]. Straggling parameters of light ions have also been evaluated by means of the LPA [16]. Furthermore, this type of approach predicts reasonable mean free paths and stopping powers of electrons and positrons in solids [17,18].

The calculation, within the dielectric formalism, of MCSs of ions in a homogeneous FEG requires a double numerical integral over wave number and angular frequency, and additional integrals over the spatial coordinates must be done to apply the LPA. Triple integrals are needed even in the favorable circumstance of a spherically symmetric electron density. In this context, analytical approximations for the low- and high-energy MCSs of the homogeneous FEG facilitate largely the numerical computations.

The purpose of the present work is to improve, in a systematic way, upon the analytical expressions previously suggested for the mean free path [19], stopping power [1, 19, 20] and straggling parameter [21] of a slow bare ion moving in a homogeneous FEG. More specifically, the study of the asymptotic behaviors of the exact low-velocity MCSs at high and low electron densities allows us to develop simple analytical formulas that are in much better agreement with the exact numerical results than those employed hitherto.

2. Macroscopic cross sections in the dielectric formalism

Let us consider the slowing down of a bare ion of mass $M \gg m_e$ and charge Z_{1e} (m_e and e are the electron mass and the elementary charge, respectively) moving with velocity v in a homogeneous FEG of density n_e [Fermi wave number $k_F = \left(3\pi^2 n_e\right)^{1/3}$]. We are interested in the MCSs, which determine the moments of the energy-loss distribution after a certain path length (see e.g. [22]). Within the dielectric formalism, the MCSs are given by (see e.g. [1,3])

$$\sum_n v = \frac{2Z_1^2 e^2}{\pi \hbar v^2} \int_0^\infty \frac{dk}{k} \int_0^{kv} \mathrm{Im}\left[\frac{-1}{\varepsilon(k,\omega)}\right] (\hbar\omega)^n \, d\omega \tag{1}$$

with $n = 0,1,2,\ldots$, where $\varepsilon(k,\omega)$ is the complex dielectric function of the FEG, which depends on the wave number k and angular frequency ω of the electromagnetic disturbance caused by the passing projectile. The dimensions of Z_n are (energy)^n/length. In particular, Z_0, Z_1 and Z_2 are equal to the inverse mean free path λ^{-1}, the electronic stopping power S and the straggling parameter Ω^2, respectively.

2.1. Macroscopic cross sections in the dielectric formalism

In the present article, we deal with slow ions, i.e. such that *v* is small compared to the Fermi velocity $v_F = \hbar k_F / m_e$ of the FEG. Having recourse to the Lindhard dielectric function obtained within the

random-phase approximation (1, 3), the general expression for the low-velocity MCSs becomes

$$\sum\nolimits_n \upsilon = \frac{2Z_1^2}{(n+2)a_0}\left[\frac{2}{\pi}E_h(\upsilon/\upsilon_0)\right]^n C_n(x^2), \tag{2}$$

where $a_0 = \hbar/m_e e^2$ and $\upsilon_0 = e^2/\hbar$ are the Bohr radius and Bohr velocity, respectively, $E_h = m_e e^4/\hbar^2$ is the Hartree energy and

$$C_n(x^2) = \frac{1}{x^{2(n-1)}}\int_0^1 \frac{z^{n+2}dz}{\left[z^2 + x^2 f(z)\right]^2} \tag{3}$$

with

$$f(z) = \frac{1}{2} + \frac{1-z^2}{4z}\ln\left|\frac{1+z}{1-z}\right|. \tag{4}$$

In these definitions $x^2 = (\pi k_F a_0)^{-1} = (4/9\pi^4)^{1/3} r_s$ is the Lindhard parameter of the FEG with the one-electron radius r_s whereas $z = k/2k_F$ stands for the dimensionless wave number (1, 3). We can draw a parallel between the stopping power, which is actually a stopping force, of a slow ion in a FEG and the frictional (or drag) force experienced by a spherical object that moves at low speed through a viscous fluid since both forces are proportional to the projectile's velocity. Hence, we shall refer to the dimensionless quantities $C_n(x^2)$ as "friction coefficients" (this name is assigned to $Q \equiv S/\upsilon$ in non-perturbative formalisms).

The low-velocity approximation (2) implies that $\sum_n(\upsilon) \propto \upsilon^n$, as confirmed by many experiments (see e.g. the latest ones (23–25)). On the other hand, the dependence of $\sum_n(\upsilon)$ on the density of the FEG appears exclusively in $C_n(x^2)$, which may be evaluated either exactly by calculating numerically the integral (3) or by resorting to the approximations described below. For this purpose, we need to study briefly the asymptotic regimes of Eq. (3) at high and low densities of the FEG. When $x \ll 1$, i.e. at high electron densities, it is convenient to make the replacement $z \to xz$ in Eq. (3). It is then seen that when $x \ll 1$, only small arguments of the function $f(z)$ contribute to $C_n(x^2)$. Therefore, in Eq. (3) we substitute for $f(z)$ the first two terms in a series expansion in powers of z^2, i.e.

$$f(z) = 1 - \frac{z^2}{3} - \frac{z^4}{15} + O(z^6) \tag{5}$$

and straightforward integration yields the asymptotic expressions:

$$C_0(x^2) = x\left[\frac{\pi}{4} - x + \frac{\pi}{8}x^2 + \frac{\pi}{6}x^3 + O(x^4)\right] \tag{6}$$

$$C_1(x^2) = \ln\frac{1}{x} - \frac{1}{2} + \frac{2}{3}x^2\left(\ln\frac{1}{2x} + \frac{19}{12}\right) + O(x^4) \tag{7}$$

$$C_2(x^2) = \frac{1}{x^2}\left[1 - \frac{3\pi}{4}x + \left(3 + \frac{\pi^2}{4}\right)\frac{x^2}{2} - \frac{5\pi}{8}x^3 + O(x^{-4})\right] \tag{8}$$

for $x \ll 1$,

$$C_n(x^2) = \frac{1}{x^{2n+2}}\left[y_n^{(1)} - y_n^{(2)}x^{-2} + O(x^{-4})\right] \tag{9}$$

for $x \gg 1$, where the constants

$$y_n^{(m)} = m\int_0^1 \frac{z^{n+2m}dz}{\left[f(z)\right]^{m+1}}, \quad m = 1, 2, \ldots \tag{10}$$

are determined by numerical integration and are listed in Table 1.

Table 1. Numerical constants related to the exact – $C_n(x^2)$ and approximate – $C_n^{1p}(x^2)$ and $C_n^{2p}(x^2)$ friction coefficients introduced in the text.

N	$C_n(x^2)$	$C_n^{1p}(x^2)$	$C_n^{2p}(x^2)$
0	$y_0^{(1)} = 0.65084279826$ $y_0^{(2)} = 1.39522562221$	$c_0^{(0)} = \frac{1}{3}$ $c_0^{(\infty)} = 0.43256373526$ $U_0 = 0.04667916590$	$a_0^{(0)} = \frac{1}{3}$ $a_0^{(\infty)} = 0.3667202279$ $V_0 = 0.02846709334$ $b_0 = \frac{1}{12}$
1	$y_1^{(1)} = 0.52827848933$ $y_2^{(2)} = 1.24273448126$	$c_1^{(0)} = \frac{1}{3}$ $c_1^{(\infty)} = 0.43710173570$ $U_1 = 0.04170410918$	$a_1^{(0)} = \frac{1}{3}$ $a_1^{(\infty)} = 0.36098063595$ $V_1 = 0.02447936741$ $b_1 = \frac{5}{9} - \frac{2}{3}\ln 2$

2	$y_2^{(1)} = 0.44855485283$ $y_2^{(2)} = 1.12455578355$	$c_2^{(0)} = \frac{\pi^2}{16} - \frac{1}{4}$ $c_2^{(\infty)} = 0.44083236772$ $U_2 = 0.03765492326$	$a_2^{(0)} = \frac{1}{3}$ $a_2^{(\infty)} = 0.35704393019$ $V_0 = 0.02174937433$ $b_0 = \frac{3\pi^2}{16} - \frac{7}{4}$

2.2. Approximate one-parameter expressions for $C_n(x^2)$

Various approximate analytical expressions for the $C_n(x^2)$ coefficients can be achieved by setting

$$f(z) = 1 - cz^2 \tag{11}$$

in the definition of $C_n(x^2)$, where *c* is some numerical constant. Inserting Eq. (11) in (3) we obtain

$$C_0^{1p}(x^2) = \frac{x}{2\xi}\left[\frac{1}{\sqrt{|\xi|}}\, g\left(\frac{\xi}{x^2}\right) - \frac{x}{\bar{\xi}}\right] \tag{12}$$

$$C_1^{1p}(x^2) = \frac{1}{2\xi^2}\left[\ln\left(\frac{\bar{\xi}}{x^2}\right) - \frac{\xi}{\bar{\xi}}\right] \tag{13}$$

$$C_2^{1p}(x^2) = \frac{1}{2x^2\xi^2}\left[2 + \frac{x^2}{\bar{\xi}} - \frac{3x}{\sqrt{|\xi|}}\, g\left(\frac{\xi}{x^2}\right)\right] \tag{14}$$

with $\bar{c} = 1 - c, \xi = 1 - cx^2, \bar{\xi} = 1 + \bar{c}x^2$, and

$$g(x) = \begin{cases} \frac{1}{2}\ln\left|\frac{1+\sqrt{|x|}}{1-\sqrt{|x|}}\right| & if \;\; x < 0 \\ \arctan\sqrt{x} \;\; if \;\; x \geq 0 \end{cases}. \tag{15}$$

Equations (12)–(14) are finite at $x^2 = 1/c$ with $C_n^{1p}(1/c) = c^{n+1}/(n+3)$ $(n = 0,1,2)$. Equation (13) also implies that the constant *c* must be chosen such that $c < 1 + x^{-2}$. The simplest approximation for the $C_n^{2p}(x^2)$ coefficients is accomplished by setting $c = c_{R1} \equiv 0$ (i.e. $f(z) \equiv 1$) in (12)–(14). This was done by Ritchie (19) for $n = 0$ and $n = 1$, and he also proposed making the substitution $c = c_{R1} \equiv 0$; we denote the resulting coefficients as $C_n^{R1}(x^2)$ and $C_n^{R2}(x^2)$, respectively. Notice that Eq. (11) with $c = 1/2$ agrees with the exact relation $f(1) = 1/2$ [see Eq. (4)]. Lindhard and Winther (1) started

from the Taylor expansion of $f(z)$ to the order z^2 [see Eq. (5)] and took $c = c_{LW} \equiv 1/3$. The resulting coefficients shall be denoted as $C_n^{LW}(x^2)$. Later on, the same $c = c_{LW}$ approximation was adopted by Sigmund and Fu (21) to estimate the friction coefficient for the straggling parameter, Eq. (14), when $x^2 < 3$. Notice that Eq. (14) differs from the definition in (21) by a factor x^2.

It is also important to compare the approximate expressions (12)–(14) with the exact asymptotic behaviors (6)–(9). From (12)–(14) one gets

$$C_0^{1p}(x^2) = x\left[\frac{\pi}{4} - x + \frac{3\pi c}{8}x^2 + \frac{2}{3}(1-3c)x^3\right] \tag{16}$$

$$C_1^{1p}(x^2) = \ln\frac{1}{x} - \frac{1}{2} + 2x^2\left[c\ln\frac{1}{x} + \frac{1}{4}(2-3c)\right] \tag{17}$$

$$C_2^{1p}(x^2) = \frac{1}{x^2}\left[1 - \frac{3\pi}{4}x + 2(1+c)x^2 4 - \frac{15\pi c}{8}x^3\right], \tag{18}$$

when $x \ll 1$ and

$$C_0^{1p}(x^2) = \frac{1}{2cx^2}\left\{\frac{1}{c} - \frac{1}{2\sqrt{c}}\ln\left|\frac{1+\sqrt{c}}{1-\sqrt{c}}\right| - \frac{1}{x^2}\left[\frac{3}{4c^{3/2}}\ln\left|\frac{1+\sqrt{c}}{1-\sqrt{c}}\right| + \frac{1}{\bar{c}^2} - \frac{3}{2c\bar{c}}\right] + O(x^{-4})\right\} \tag{19}$$

$$C_1^{1p}(x^2) = \frac{1}{2c^2x^4}\left\{\ln\bar{c} + \frac{c}{\bar{c}} - \frac{1}{x^2}\left[\frac{2}{c}\ln\frac{1}{\bar{c}} - \frac{2-3c}{\bar{c}^2}\right] + O(x^{-4})\right\} \tag{20}$$

$$C_2^{1p}(x^2) = \frac{1}{2c^2x^6}\left\{2 + \frac{1}{\bar{c}} - \frac{3}{2\sqrt{c}}\ln\left|\frac{1+\sqrt{c}}{1-\sqrt{c}}\right| - \frac{1}{x^2}\left[\frac{15}{4c^{3/2}}\ln\left|\frac{1+\sqrt{c}}{1-\sqrt{c}}\right| + \frac{1}{\bar{c}^2} - \frac{3}{2c\bar{c}} - \frac{4}{c}\right] + O(x^{-4})\right\}, \tag{21}$$

when $x \gg 1$. Comparison of (16)–(18) with equations (6)–(8) reveals that the first and second terms of these expressions coincide (regardless of c) while the other terms may differ from each other. For instance, assuming that $c = c_{LW} \equiv 1/3$ the approximate equations (16) and (17) are correct (cf. expressions (6) and (7), respectively) up to the orders $O(x^3)$ and $O(x^2\ln x)$, respectively. The deviations of the numerical constants in the fourth term of Eq. (17) and in the third term of Eq. (18) from the corresponding constants in (7) and (8) are $5/6 - \ln 2 \simeq 0.14$ and $\pi^2/8 - 7/6 \simeq 0.07$. Similarly, at low densities equations (19)–(21) can be represented in the asymptotic form (9), with expansion coefficients $y_n^{(1)LW}$ and $y_n^{(2)LW}$ which, in general, differ somewhat from the exact $y_n^{(1)}$ and $y_n^{(2)}$ values in Table 1. Thus, in the case of C_1 we have $y_n^{(1)LW} = 0.42540701351$ and $y_1^{(2)LW} = 0.82255791892$, and the departure from the exact values of Table 1 is apparent.

As we have seen, $C_n^{Rl}(x^2)$, $C_n^{R2}(x^2)$ and $C_n^{LW}(x^2)$ rely only on the approximation $f(z)=1-cz^2$ and just differ in the choice of the constant c. To improve the approximation (13) for the stopping power friction coefficient, (20) deduced the constant c by equating the $O(x^{-4})$ term of Eq. (20) with the first term, $y_1^{(1)}x^{-4}$, of the exact asymptotic relation (9). The solution of the resulting transcendental equation for the constant c is $c_{FA}=0.427$, and it lies between $c_{LW}=1/3$ and $c_{R2}=1/2$. With c_{FA} the approximation (13) for the $n=1$ friction coefficient, denoted as $C_1^{FA}(x^2)$, is greatly improved compared to the cases with constants c_{Rl}, c_{R2} or c_{LW} (20).

For further improvement of the approximate expressions (12)–(14) we adjust here the constant c_n for each n (with $n=0,1,2,...$) so as to be in agreement with the exact asymptotic relations (6)–(8) and (9) at $x\ll 1$ and $x\gg 1$, respectively, and up to the orders $O(x^2\ln x)$ and $O(x^{-(2n+4)})$. It is clear that this is only possible if $c=c_n(x^2)$ is treated as a function of n and the density parameter x^2 of the FEG. From the structures of the asymptotic formulas (6)–(9) and (16)–(21) it follows that the desired quantities $c_n(x^2)$ should behave as

$$c_n(x^2)=c_n^{(0)}+O(x^2)\,;\quad x\ll 1 \tag{22}$$

$$c_n(x^2)=c_n^{(\infty)}-U_n x^{-2}+O(x^{-4})\,;\quad x\gg 1, \tag{23}$$

where U_n, $c_n^{(0)}$ and $c_n^{(\infty)}$ are constants. In contrast to (20) three relations are needed here to determine these constants. For instance, from Eq. (17) with the asymptotic behavior (22) it ensures that

$$C_1^{1p}(x^2)=\ln\frac{1}{x}-\frac{1}{2}+2x^2\left[c_1^{(0)}\ln\frac{1}{x}+\frac{1}{4}(2-3c_1^{(0)})\right] \tag{24}$$

Comparison of (24) with the exact equation (7) shows that the latter cannot be exactly satisfied for any $c_1^{(0)}$. However, choosing the value $c_i^{(0)}=1/3$ it is fulfilled up to the leading $O(x^2\ln x)$ (logarithmic) order. Analogously, comparing (16) and (18) with equations (6) and (8), respectively, and taking into account the relation (22) we get $c_0^{(0)}=1/3$ and $c_2^{(0)}=\pi^2/16-1/4$. These numerical constants satisfy the exact relations (6) and (8) up to the orders $O(x^3)$ and $O(1)$, respectively.

Next, similar calculations can be done inserting Eq. (23) into (19)–(21) and keeping only the terms up to the order $O(x^{-(2n+4)})$. Comparing now the $O(x^{-(2n+2)})$ and $O(x^{-(2n+4)})$ terms of the resulting equations with the corresponding ($y_n^{(1)}x^{-(2n+2)}$ and $y_n^{(2)}x^{-(2n+4)}$) terms of (9) we obtain a set of transcendental equations for the unknown quantities U_n and $c_n^{(\infty)}$ with $n=0, 1, 2$

$$\frac{1}{2c_0^{(\infty)}}\left[\frac{1}{1-c_0^{(\infty)}}-\frac{\ln\, p_0}{2[c_0^{(\infty)}]^{1/2}}\right]=y_0^{(1)} \tag{25}$$

$$\frac{1}{2[c_1^{(\infty)}]^2}\left[\ln(1-c_1^{(\infty)})-\frac{c_1^{(\infty)}}{1-c_1^{(\infty)}}\right]=y_1^{(1)} \tag{26}$$

$$\frac{1}{2[c_2^{(\infty)}]^2}\left[\frac{3-2c_2^{(\infty)}}{1-c_2^{(\infty)}}-\frac{3\ln\, p_2}{2[c_2^{(\infty)}]^{1/2}}\right]=y_2^{(1)} \tag{27}$$

and

$$\frac{U_0+1}{2[c_0^{(\infty)}]^2}\left[\frac{3\ln\, p_0}{4[c_0^{(\infty)}]^{1/2}}-\frac{5c_0^{(\infty)}-3}{2(1-c_0^{(\infty)})^{1/2}}\right]=y_0^{(2)} \tag{28}$$

$$\frac{U_1+1}{[c_1^{(\infty)}]^3}\left[\frac{c_1^{(\infty)}(3c_1^{(\infty)}-2)}{2(1-c_1^{(\infty)})^2}-\ln(1-c_1^{(\infty)})\right]=y_1^{(2)} \tag{29}$$

$$\frac{U_2+1}{2[c_2^{(\infty)}]^3}\left[\frac{15\ln\, p_2}{4[c_0^{(\infty)}]^{1/2}}+\frac{9c_2^{(\infty)}-7}{2(1-c_2^{(\infty)})^2}-4\right]=y_2^{(2)}\,. \tag{30}$$

Here $p_n=\{1+[c_n^{(\infty)}]^{1/2}\}/\{1-[c_n^{(\infty)}]^{1/2}\}$ with $n=0,2$. The set of equations (25)–(27) contains only the quantities $c_n^{(\infty)}$ and yields the numerical solution provided in Table 1. [Equation (26) for the quantity $c_1^{(\infty)}$ has been previously deduced in (20), and its solution is the aforementioned value $c_1^{(\infty)}=c_{FA}=0.437$]. Then, the expansion coefficients Un of Eq. (23) are determined inserting the constants $c_n^{(\infty)}$ into (28)–(30). The numerical values of these solutions are included in Table 1.

The asymptotic expressions (22) and (23) thus suggest to evaluate $c_n(x^2)$ by an interpolation between $c_n^{(0)}$ at $x\ll 1$ and $c_n^{(\infty)}$ at $x\gg 1$, which then covers the entire range of variation of the density parameter x^2, from the high-density to the low-density regimes. To this end, we propose the simple

interpolation formula

$$c_n(x^2) = c_n^{(\infty)} - \frac{U_n}{x^2 + U_n / (c_n^{(\infty)} - c_n^{(0)})}. \tag{31}$$

The accuracy of the approximations (12)–(14) together with Eq. (31) will be analyzed in section 3.

2.3. Approximate two-parameter expressions for $C_n(x^2)$

More accurate analytical expressions for the coefficients $C_n(x^2)$ can be elaborated if the function $f(z)$ in (3) is approximated in the form

$$f(z) = 1 - az^2 - bz^4 \tag{32}$$

with two yet unknown parameters a and b. Note that a = 1/3 and b = 1/15 in the case of the Taylor series expansion of the function $f(z)$, see Eq. (5). With this choice for the function $f(z)$ following the same mathematical steps that led to (12)–(14), we now get

$$C_0^{2p}(x^2) = \frac{x^2}{2A^2}\left[\frac{\sqrt{b}}{2\eta}\left(\frac{2\alpha}{A}+1\right)\ln\left|\frac{\sqrt{b}+\eta}{\sqrt{b}-\eta}\right| + \eta\left(\frac{2\alpha}{A}-1\right)\arctan\eta + \frac{b}{\eta^2-b} - \frac{\eta^2}{\eta^2+1}\right] \tag{33}$$

$$C_1^{2p}(x^2) = \frac{1}{A^2}\left\{\frac{\alpha}{A}\ln\frac{\left|A+\alpha+2x^2\right|}{2x\sqrt{|\gamma|}} - \frac{\beta}{2\gamma}\right\} \tag{34}$$

$$C_2^{2p}(x^2) = \frac{1}{2x^2A^2}\left\{\frac{1}{2\eta\sqrt{b}}\left[\frac{\alpha}{x^2} + b\left(\frac{1}{\eta^2} - \frac{4x^2}{A}\right)\right]\ln\left|\frac{\sqrt{b}+\eta}{\sqrt{b}-\eta}\right| \right. \tag{35}$$

$$\left. -\frac{1}{\eta}\left(\frac{2\alpha}{A}+1\right)\arctan\eta + \frac{1}{\eta^2+1} + \frac{\alpha\eta^2 + bx^2}{x^2\eta^2(\eta^2-b)}\right\},$$

where

$$\alpha = 1 - ax^2,\ \beta = 1 - Hx^2,\ \gamma = 1 + g^2x^2,$$
$$A = \sqrt{\alpha^2 + 4bx^2},\ \eta = \sqrt{\frac{A+\alpha}{2x^2}} \tag{36}$$

with $H = a + 2b,\ g = \sqrt{1-a-b}$. It is easy to see that equations (33)–(35) with $a = c$ and $b = 0$ agree with (12)–(14).

Consider now the asymptotic expansions of equations (33)–(35). For instance, from (34) it follows that

$$C_1^{2p}(x^2) = \ln\frac{1}{x} - \frac{1}{2} + 2x^2\left[a\ln\frac{1}{x} + \frac{1}{2}\left(1 + b - \frac{3}{2}a\right)\right], \tag{37}$$

when $x \ll 1$ and

$$C_1^{2p}(x^2) = \frac{1}{x^4 h^2}\left\{\frac{H}{2g^2} - \frac{a}{h}\ln\left(\frac{h+H}{g(h+a)}\right)\right. \tag{38}$$
$$\left. - \frac{1}{x^2}\left[\frac{a\left(a^2-2b\right)}{h^3}\ln\left(\frac{h+H}{g(h+a)}\right) + \frac{1}{2g^2}\left(\frac{1+b}{g^2} - \frac{3aH}{h^2}\right)\right]\right\},$$

when $x \gg 1,$ where $h = \sqrt{a^2+4b}$. From Eq. (37) it is seen that the exact asymptotic relation (7) can now be fulfilled exactly with two parameters a and b. Similar asymptotic expressions can be derived for the coefficients $C_0^{2p}(x^2)$ and $C_2^{2p}(x^2)$ which then satisfy the exact asymptotic relations (6) and (8) with two parameters a and b.

We will treat here the parameter $b = b_n$ as a constant with $n = 0,1,2$ whereas, as in section 2.2, the parameter a is regarded as a function of x^2 with asymptotic forms resembling equations (22) and (23)

$$a_n(x^2) = a_n^{(0)} + O(x^2);\quad x \ll 1 \tag{39}$$

$$a_n(x^2) = a_n^{(\infty)} - V_n x^{-2} + O(x^{-4});\quad x \gg 1. \tag{40}$$

Here $V_n, a_n^{(0)}$ and $a_n^{(\infty)}$ are unknown expansion coefficients. As it has been done above, we compare Eq. (37) together with the expansion (39) with the exact relation (7), which yields $a_1^{(0)} = 1/3$ and $b_1 = \frac{5}{9} - \frac{2}{3}\ln 2$ (see Table 1). An analogous procedure for the coefficients $C_0^{2p}(x^2)$ and $C_2^{2p}(x^2)$ furnishes $a_0^{(0)} = \frac{1}{3}, b_0 = \frac{1}{12}$ and $a_2^{(0)} = \frac{1}{3}, b_2 = \frac{3\pi^2}{16} - \frac{7}{4}$ (see Table 1). It can be observed that b_0, b_1 and b_2 are somewhat larger than the corresponding coefficients in the exact series expansion of $f(z)$, Eq. (5). In the opposite regime of low densities $x \gg 1$ from (38), (40) and (9) we arrive at a system of

equations for the constants V_1 and $a_1^{(\infty)}$

$$\frac{1}{h_0^2}\left[\frac{H_0}{2g_0^2}-\frac{a_1^{(\infty)}}{h_0}\left(\frac{h_0+H_0}{g_0\left(h_0+a_1^{(\infty)}\right)}\right)\right]=y_1^{(1)} \tag{41}$$

$$\frac{V_1+1}{h_0^2}\left[\frac{2([a_1^{(\infty)}]^2-2b_1)}{h_0^3}\ln\left(\frac{h_0+H_0}{g_0(h_0+a_1^{(\infty)})}\right)\right. \tag{42}$$

$$\left.\frac{1}{2g_0^2}\left(\frac{1+b_1}{g_0^2}-\frac{3a_1^{(\infty)}H_0}{h_0^2}\right)\right]=y_1^{(2)},$$

where $g_0=\left[1-a_1^{(\infty)}-b_1\right]^{1/2}, h_0=\{[a_1^{(\infty)}]^2+4b_1\}^{1/2}, H_0=a_1^{(\infty)}+2b_1$ with the numerical solutions listed in Table 1. The derivation of equivalent equations for $V_0, a_0^{(\infty)}$ and $V_2, a_2^{(\infty)}$ are straightforward. The solutions of these latter equations are also summarized in Table 1.

Finally, to cover the entire range of variation of the density parameter x^2 , from the high density to the low-density regimes, we propose the interpolation formula [cf. Eq. (31)]

$$a_n(x^2)=a_n^{(\infty)}-\frac{V_n}{x^2+V_n/(a_n^{(\infty)}-a_n^{(0)})}, \tag{43}$$

which ensures the correct behaviors of (43) at $x\ll 1$ and $x\gg 1$.

3. Results and discussion

The "classical" formulas $C_n^{R1}(x^2)$, $C_n^{R2}(x^2)$ and $C_n^{LW}(x^2)$, calculated from (12)–(14) with $c=0, c=1/2$ and $c=1/3$, respectively, are shown in Figure 1 for $n=0,1$ and 2. The plotted quantities are actually the ratios of these functions to the exact friction coefficients, Eq. (3) with $n=0,1$ and 2. In addition, Figure 1 includes the ratios pertaining to the two-parameter approximations $C_0^{2p}(x^2)$, $C_1^{2p}(x^2)$ and $C_2^{2p}(x^2)$, calculated by means of equations (33)–(35) with $a=1/3$ and $b=1/15$ as dictated by the exact series expansion (5).

The approximate coefficients $C_n^{R1}(x^2)$, $C_n^{R2}(x^2)$ and $C_n^{LW}(x^2)$ (with $n=0,1,2$) depicted in Figure 1 tend to the exact numerical results when $x\ll 1$. This is because the leading order terms of equations (6)–(8) are reproduced by (16)–(18) regardless of the parameter c. On the other hand, the latter equations do not fulfill the asymptotic behavior (9) at small densities, which leads to large deviations from the exact values at $x\gg 1$: the relative errors of the R2 and LW approximations reach 15% to 21%. The simpler R1 approximation exhibits the same trends, but the relative errors are about 50% when $x\to\infty$. These high- and low-density behaviors are also seen in the case of the two-parameter

approximations (33)–(35) with $a = 1/3$ and $b = 1/15$. However, the coefficients $C_n^{2p}(x^2)$ with $n = 0,1$ and 2 are improved, albeit only moderately because the relative deviations are still in the range 9% to 11%.

Equations (12)–(14) and (33)–(35) with the respective interpolation formulas (31) and (43) constitute the main results of this paper. Figures 2, 3 and 4 display, respectively, the approximate friction coefficients $C_n^{1p}(x^2)$ and $C_n^{2p}(x^2)$ calculated with these equations for n = 0, 1, and 2, divided by the corresponding exact $C_n(x^2)$ functions.

All approximate expressions shown in Figures 2–4 have relative errors that diminish with either decreasing or increasing electron densities because they reproduce in both limits the exact asymptotic behaviors (6)–(9). In particular, $C_1^{FA}(x^2)$ (see Figure 3) reproduces at x<<1 and x>>1 the leading $O(\ln x)$ and $O(x^{-4})$ terms of equations (7) and (9), respectively; the largest relative departure is 2%. The approximations $C_1^{1p}(x^2)$ and $C_1^{2p}(x^2)$ yield, in addition, the $O(x^2 \ln x)$ and $O(x^{-6})$ terms, which improves substantially the overall agreement with the exact $C_1(x^2)$ coefficient. As a consequence, the largest relative errors of $C_1^{1p}(x^2)$ and $C_1^{2p}(x^2)$ are reduced to 0.75% and 0.09%, respectively (see Figure 3). Furthermore, the maximum deviations of $C_0^{1p}(x^2)$, $C_0^{2p}(x^2)$, $C_2^{1p}(x^2)$ and $C_2^{2p}(x^2)$ from the corresponding exact values are 0.53%, 0.1%, 0.5% and 0.08%, respectively (see Figures 2 and 4). We conclude that the proposed analytical coefficients $C_n^{1p}(x^2)$ and $C_n^{2p}(x^2)$ are very accurate, especially at typical densities of conduction electrons in metals, $x^2 \approx 0.25 (r_s \approx 1.5-6)$.

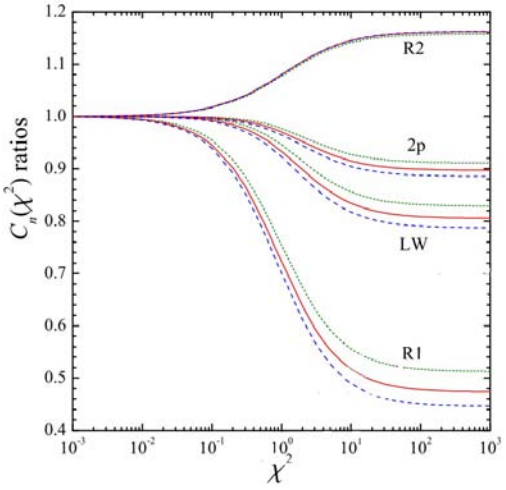

Fig. 1. Ratios of the coefficients $C_n^{R1}(x^2)$, $C_n^{R2}(x^2)$ and $C_n^{LW}(x^2)$ (n = 0, 1, 2) calculated using equations (12)–(14) with c = 0, c = 1/2 and c = 1/3, respectively, to the respective exact $C_n(x^2)$ (Eq. (3) with n = 0, 1, 2). The dotted, solid and dashed curves correspond to n = 0, 1 and 2, respectively. The curves labeled with the abbreviation 2p are the ratios pertaining to $C_n^{2p}(x^2)$ (n = 0, 1, 2), calculated using the two-parameter approximations (33)–(35) with a = 1/3 and b = 1/15.

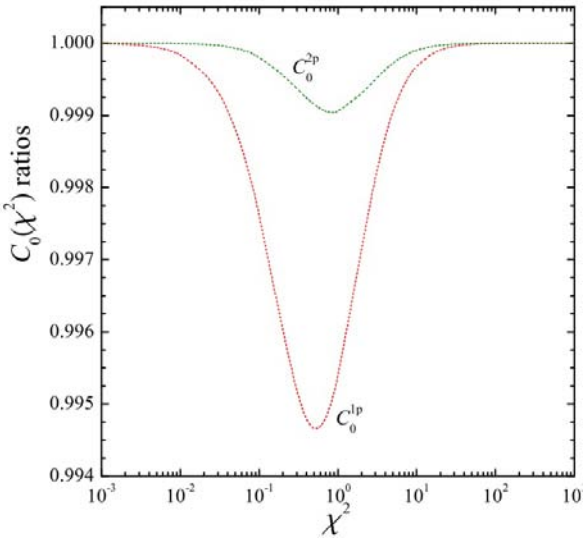

Fig. 2. Ratios of the coefficients $C_0^{1p}(x^2)$ and $C_0^{2p}(x^2)$ calculated with equations (12), (31) and (33), (43), respectively, to the exact $C_0(x^2)$ (Eq. (3) with n = 0).

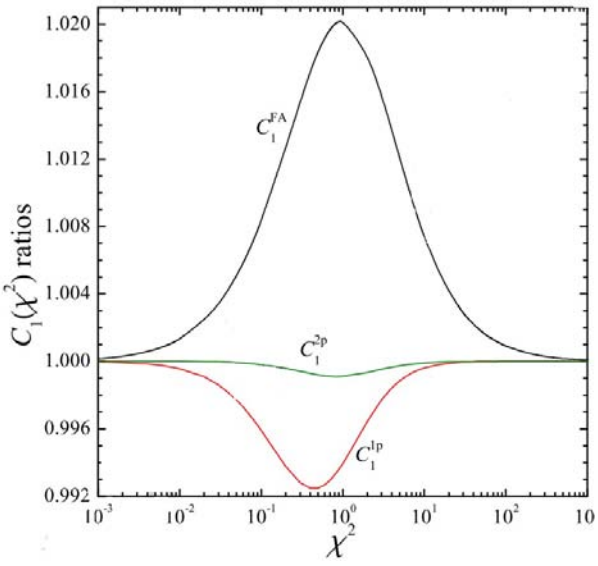

Fig. 3. Ratios of the coefficients $C_1^{1p}(x^2)$ and $C_1^{2p}(x^2)$ calculated with equations (13), (31) and (34), (43), respectively, to the exact $C_1(x^2)$ (Eq. (3) with n = 1). The ratio of the coefficient $C_1^{FA}(x^2)$, Eq. (13) with $c = c_{FA} = c_1^{(\infty)}$, to the exact $C_1(x^2)$ function is also plotted.

Before concluding this section, we would like to make a couple of remarks. Figures 1–4 display the friction coefficients in the interval of $10^{-3} \le x^2 \le 10^3$. However, for very high densities approaching, $x^2 = e^2/\pi\hbar c = 2.3\times10^{-3}$ the Fermi velocity of the FEG becomes comparable to the speed of light and the FEG turns relativistic (26). On the other hand, the FEG undergoes a transition to a Wigner crystal at $r_s \approx 106$, i.e. $x^2 = 17.6$ (27) (see also (28)). Therefore, the applicability of the present analytical results is restricted to $2.3\times10^{-3} < x^2 < 17.6$.

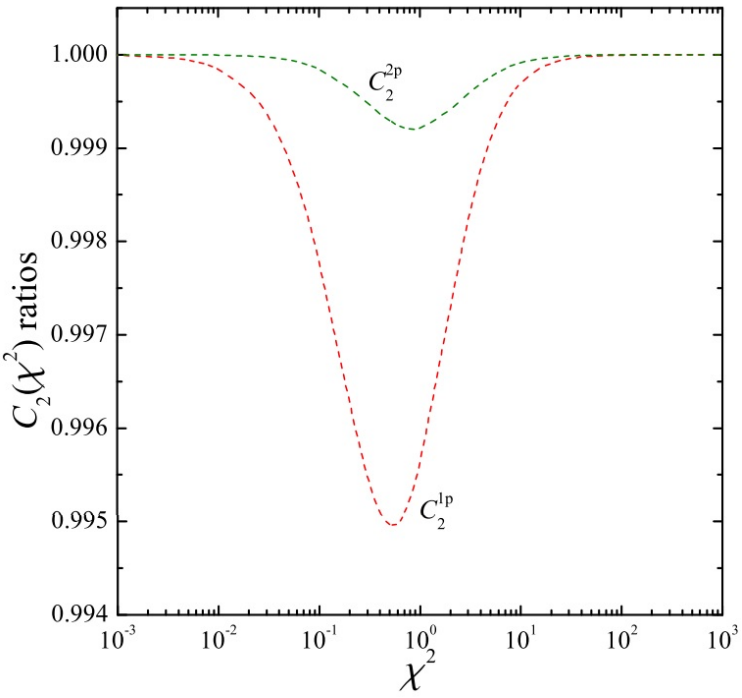

Fig. 4. Ratios of the coefficients $C_2^{1p}(x^2)$ and $C_2^{2p}(x^2)$ calculated with equations (14), (31) and (35), (43), respectively, to the exact $C_2(x^2)$ (Eq. (3) with $n = 2$).

6. Conclusion

Various analytical expressions for the inverse mean free path, the stopping power and the straggling parameter of slow bare ions moving in a FEG of constant density have been considered. Approximate formulas for the friction coefficients $C_n(x^2)$ that appear in the definition of these MCSs have been proposed. As in the previous approaches (1, 19–21) one of these formulas is based on the approximation $f(z) = 1 - cz^2$ in the definition of $C_n(x^2)$, with the single parameter c adjusted to yield the correct asymptotic behaviors both in the high- and low density limits. Besides, we have

studied the performance of the two-parameter approximation $f(z)=1-az^2-bz^4$, with the two unknown parameters a and b adjusted in a similar manner [or fixed to the values dictated by the Taylor expansion of $f(z)$]. In the case of the stopping power friction coefficient it has been shown that both approximations are notably more precise than those of (1, 19, 20). In turn, the developed approximations for $C_0(x^2)$ and $C_2(x^2)$ are highly accurate when compared to the results of (19) and (21), respectively. The largest errors of the suggested one- and two-parameter approximations do not exceed 0.8% and 0.1%, respectively. Going beyond the present model of the FEG we can envisage a number of improvements. For instance, exchange-correlation effects are important at metallic densities and can be included via a local-field correction to the dielectric function. The corresponding friction coefficients may be found by repeating the same steps that led to the results of sections 2.1–2.3. In addition to the limitations indicated at the end of section 3 it should be recalled that the present analysis is valid in the low-velocity limit of the ion, i.e. $v<v_F$. In addition, since $v_F \propto x^{-2}$, the low-velocity regime requires smaller ion velocities when the density of the FEG decreases. In these circumstances one should care about ion recoil effects, non-linear effects in the electron scattering, and possible quantum properties of the projectile when its de Broglie wavelength becomes comparable to the inter particle distances.

Fortunately, the aforementioned shortcomings of the dielectric formalism in the random-phase approximation are greatly suppressed when the LPA together with the dielectric formalism is applied to real solids. On one hand, the smallest local electron densities are found in the interstitial regions between atoms and are typically $x^2 \le 1$. On the other hand, in the constrained LPA (29) the excitation of deep core electrons is either neglected or treated separately, limiting in practice the domain where the LPA has to be employed to $x^2 \ge 1$. Therefore, the present analytical results may be useful for quick estimates of the mean free path, stopping power and straggling parameter of slow ions in solids.

This work was supported by the RA MES State Committee of Science in the framework of the research project № 15T-1C231.

References

[1] Echenique, P.M.; Flores, F.; Ritchie, R.H. Solid State Phys. 1990, 43, 229–308.
[2] Sigmund, P. Particle Penetration and Radiation Effects; Springer: Berlin, 2006.
[3] Lindhard, J. K. Dan. Vidensk. Selsk. Mat.-Fys. Medd. 1954, 28, 1.
[4] Lindhard, J.; Winther, A. K. Dan. Vidensk. Selsk. Mat.-Fys. Medd. 1964, 34, 1.
[5] Nersisyan, H.B.; Das, A.K. Phys. Rev. E 2004, 69, 046404.
[6] Nersisyan, H.B.; Das, A.K. Interaction of ion beams with plasmas: Energy loss and equipartition sum rules, Advances in Plasma Physics Research, vol. 6, chapter 2, pp. 81–125, edited by F. Gerard, Nova Science: New York, 2008.
[7] Johnson, R.E.: Inokuti, M. Comments At. Mol. Phys. 1983, 14, 19–31.
[8] Arista, N.R. J. Phys. C: Condens. Matter 1986, 19, L841–L845.
[9] Ascolani, H.: Arista, N.R. Phys. Rev. A 1986, 33, 2352–2357.

[10] Bonderup, E. K. Dan. Vidensk. Selsk. Mat.-Fys. Medd. 1967, 35, 17.
[11] Chu, W.K.: Moruzzi, V.L.: Ziegler, J.F. J. Appl. Phys. 1975, 46, 2817–2820.
[12] Gertner, I.: Meron, M.: Rosner, B. Phys. Rev. A 1978, 18, 2022–2029.
[13] Gertner, I.: Meron, M.: Rosner, B. Phys. Rev. A 1980, 21, 1191–1196.
[14] Iafrate, G.J.: Ziegler, J.F.: Nass, M.J. J. Appl. Phys. 1980, 51, 984–987.
[15] Rousseau, C.C.: Chu, W.K.: Powers, D. Phys. Rev. A 1971, 4, 1066–1070.
[16] Ziegler, J.F.: Chu, W.K. At. Data Nucl. Data Tables 1974, 13, 463–489.
[17] van Dijk, P.W.L.: van Ijzendoorn, L.J.: de Koning, M.: Bobbert, P.: van Haeringen, W.: de Voigt, M.J.A. Nucl. Instrum. Methods B 1994, 85, 551–555.
[18] Sarasola, A.: Ponce, V.H.: Arnau, A. Nucl. Instrum. Methods B 2003, 203, 104–110.
[19] Chu, W.K. Phys. Rev. A 1976, 13, 2057–2060.
[20] Mayol, R.: Fernandez-Varea, J.M.: Salvat, F.: Liljequist, D. Inelastic interactions of electrons with solids: LPA ´ and Penn's statistical model (Interaction of Charged Particles with Solids and Surfaces, NATO ASI Series vol. B-271), edited by A. Gras-Mart´ı, H.M. Urbassek, N.R. Arista, F. Flores, Plenum Publishing: New York, 1991, pp. 585–591.
[21] Tung, C.J.: Ashley, J.C.: Ritchie, R.H. Surf. Sci. 1979, 81, 427–439.
[22] Ritchie, R.H. Phys. Rev. 1959, 114, 644–654.
[23] Fernandez-Varea, J.M.: Arista, N.R. ´ Radiat. Phys. Chem. 2014, 96, 88–91.
[24] Sigmund, P.: Fu, D.J. Phys. Rev. A 1982, 25, 1450–1455.
[25] Fernandez-Varea, J.M.: Mart ´ ´ınez, J.D.: Salvat, F. J. Phys. D: Appl. Phys. 1991, 24, 814–826.
[26] Møller, S.P.: Csete, A.: Ichioka, T.: Knudsen, H.: Uggerhøj, U.I.: Andersen, H.H. Phys. Rev. Lett. 2002, 88, 193201.
[27] Møller, S.P.: Csete, A.: Ichioka, T.: Knudsen, H.: Uggerhøj, U.I.: Andersen, H.H. Phys. Rev. Lett. 2004, 93, 042502.
[28] Møller, S.P.: Csete, A.: Ichioka, T.: Knudsen, H.: Kristiansen, H.-P.E.: Uggerhøj, U.I.: Andersen, H.H.: Sigmund, P.: Schinner, A. Eur. Phys. J. D 2008, 46, 89–92.
[29] Nagy, I. J. Phys. B: At. Mol. Phys. 1986, 19, L421–L426.
[30] Drummond, N.D.: Radnai, Z.: Trail, J.R.: Towler, M.D.: Needs, R.J. Phys. Rev. B 2004, 69, 085116.
[31] Nagy, I.: Echenique, P.M. Phys. Rev. B 2010, 81, 113109.
[32] Wang, N.-P.: Nagy, I.: Echenique, P.M. Phys. Rev. B 1998, 58, 2357–2360.